Plant, Cell & Environment

Plant, Cell and Environment (2012) doi: 10.1111/j.1365-3040.2011.02470.x

Changes in stomatal conductance along grass blades reflect changes in leaf structure

T. W. OCHELTREE[1,2], J. B. NIPPERT[2] & P. V. V. PRASAD[1]

[1]Department of Agronomy, Kansas State University, 2004 Throckmorton Hall, Manhattan, KS 66506, USA and [2]Division of Biology, Kansas State University, 116 Ackert Hall, Manhattan, KS 66506, USA

ABSTRACT

Identifying the consequences of grass blade morphology (long, narrow leaves) on the heterogeneity of gas exchange is fundamental to an understanding of the physiology of this growth form. We examined acropetal changes in anatomy, hydraulic conductivity and rates of gas exchange in five grass species (including C_3 and C_4 functional types). Both stomatal conductance and photosynthesis increased along all grass blades despite constant light availability. Hydraulic efficiency within the xylem remained constant along the leaf, but structural changes outside the xylem changed in concert with stomatal conductance. Stomatal density and stomatal pore index remained constant along grass blades but interveinal distance decreased acropetally resulting in a decreased path length for water movement from vascular bundle to stomate. The increase in stomatal conductance was correlated with the decreased path length through the leaf mesophyll. A strong correlation between the distance from vascular bundles to stomatal pores and stomatal conductance has been identified across species; our results suggest this relationship also exists within individual leaves.

Key-words: gas exchange; grass anatomy; grass hydraulics; hydraulic architecture; leaf hydraulic conductivity.

INTRODUCTION

Identifying the relationship between leaf structure and function across species has received considerable attention (Sack & Frole 2006; Brodribb, Feild & Jordan 2007), and has elucidated many trade-offs between water use and carbon gain. However, the relationship between structure and function within individual leaves has received less attention. Water potential gradients within individual eudicot leaves suggest that the balance between water supply and demand changes within individual leaves. In the elongate leaves of *Laurus nobilis* L., water potential decreased from the base to tip of individual leaves (Zwieniecki *et al*. 2002; Cochard, Nardini & Coll 2004), which would result in acropetal changes in cell water status. These acropetal water potential gradients would be exacerbated in long, narrow leaves (such as monocot leaves) and would likely correspond to large changes in plant behaviour across a single leaf. A better understanding of the structure and function of monocot leaves is necessary to understand changes in the balance between water loss and carbon assimilation as water is transported through the vasculature to the site of evaporation.

The heterogeneity of stomatal conductance to water vapour (g_{wv}) within individual eudicot leaves has been the focus of recent studies (Buckley & Mott 2000; Marenco *et al*. 2006; Nardini *et al*. 2008). 'Patchy' adjustments in g_{wv} appear to respond to local changes in hydraulic conductance in eudicot leaves, as xylem conduits cavitate and refill on diurnal timescales (Marenco *et al*. 2006). Localized dynamic control of g_{wv} in eudicots leads to seemingly random heterogeneity as the plant maximizes gas exchange across the entire leaf surface as the environment changes (Buckley, Farquhar & Mott 1999). Preliminary data on the heterogeneity of stomatal conductance in monocot leaves suggest a more systematic pattern; measurements made along grass blades found photosynthesis (A) increased acropetally for *Saccharum officinarum* L. (sugarcane, Meinzer & Saliendra 1997) and *Zea mays* (Miranda, Baker & Long 1981a; Long *et al*. 1989). Systematic changes in transpiration (E) along grass blades have been shown in research modelling the enrichment of ^{18}O in leaf water of grasses (Helliker & Ehleringer 2000; Affek, Krisch & Yakir 2006; Ogee *et al*. 2007). Model accuracy of ^{18}O enrichment is high only when E increased acropetally. Furthermore, Ogee *et al*. (2007) showed that all published data of ^{18}O enrichment along leaves could be accurately described assuming increases in E. Thus, while acropetal increases in E have been reported in monocots previously, most research has been limited to either *Zea mays* L. or *Saccharum officinarum* L. and the implications of increased water demand along grass blades have not been investigated.

Broadly, the structure of the hydraulic system within leaves constrains whole plant water use and correlates with maximum rates of leaf-level gas exchange. For example, the conductance to water flow through leaves has been shown to correlate positively with photosynthetic capacity (Brodribb *et al*. 2005, 2007). Furthermore, the resistance within leaves correlated strongly with the path length from vascular bundle to stomatal pore (Brodribb *et al*. 2007), suggesting that vein placement within leaves may be the limiting factor to maximum rates of gas exchange. In tropical

Correspondence: T. W. Ocheltree. e-mail: troyoch@ksu.edu

rainforest leaves, the structure of the mesophyll exerted strong controls on the movement of water through leaves; both xylem density and palisade : spongy mesophyll ratio correlated with leaf resistance to water flow (Sack & Frole 2006). These results emphasize the importance of extravascular resistances to the movement of water through leaves and maximum rates of gas exchange, at least under well-watered conditions.

Monocot leaf blades are typically long and tapering, and this shape influences the internal structure of the hydraulic pathway. As blades taper, the distance between vascular bundles decreases (Colbert & Evert 1982; Russell & Evert 1985; Dannenhoffer, Ebert & Evert 1990; Martre & Durand 2001) as fewer bundles terminate compared with the degree of tapering. The mean diameter of xylem vessels decreases, resulting in decreasing hydraulic conductivity within the xylem (K_x), but when normalized by leaf area, leaf specific K_x remains relatively constant along grass blades (Martre & Durand 2001). This is consistent with plant scaling theory for trees (West, Brown & Enquist 1999) and would minimize the pressure drop along the blade. In contrast to the changes in interveinal distances, the density of stomatal pores often remains constant along the grass blades (*Zea mays* L. – Miranda, Baker & Long 1981b). If stomatal densities remain constant and interveinal distances decrease, it then follows that the diffusional path length from vascular bundle to stomate should also change along the length of monocot leaf blades, and these changes in path length would provide a structural mechanism to facilitate corresponding changes in g_{wv}.

The objective of this study was to investigate the correlation between hydraulic architecture and rates of gas exchange within individual grass blades. We measured the hydraulic conductance, gas exchange rates and anatomical characteristics from corresponding positions within leaves of five common tallgrass prairie species. We hypothesized that: (1) *A*, *E* and g_{wv} will increase along the leaf even in the presence of constant light intensity along the leaf; (2) leaf specific K_x will remain constant along the leaf; and (3) the distance from vascular bundle to stomatal pore will decrease acropetally and will correlate with g_{wv} within individual grass blades.

MATERIALS AND METHODS

Plant tissue

Five common grass species native to the tallgrass prairie were selected for this study: *Andropogon gerardii* Vitman (*Ange*, C_4 NADP-ME), *Sorghastrum nutans* Nash (*Sonu*, C_4 NADP-ME), *Schizachyrium scoparium* Nash (*Scsc*, C_4 NADP-ME), *Elymus canadensis* L. (*Elca*, C_3) and *Bromus inermis* Leyss. (*Brin*, C_3). C_3 and C_4 species were included in this study to investigate the generality of the patterns across a range of grass species rather than an attempt to characterize differences between these functional groups. Leaf characteristics of the measured species are shown in Table 1. Seeds were collected from Konza Prairie Biological Station, Kansas, USA (KPBS) and stored at 4 °C until the initiation of the study. Seeds of each species were germinated on wet filter paper and then five individuals were transplanted into 1.65 L pots ('Short One' Treepots; Stuewe & Sons, Inc., Tangent, OR, USA) filled with soil taken from KPBS. This resulted in five replicates per species, which were then randomly distributed within a growth chamber (Conviron PGV 36; Conviron Environments Limited, Winnipeg, Manitoba, Canada). Air temperature in the growth chamber was maintained at 30 °C with a 16 h photoperiod. The light intensity at the top of the canopy was maintained at ~1000 μmol m^{-2} s^{-1} by adjusting the height of the lights as the canopy grew. Plants were watered daily to ensure that soil moisture remained near pot-holding capacity. Plants were grown until they had four to six mature leaves before beginning measurements. On day 1 of a measurement cycle, three plants were randomly selected across all species and gas exchange measurements were made on one leaf per plant. After the photoperiod ended on that same day, plants were covered with a plastic bag and placed in a dark enclosure to allow leaves to fully hydrate for hydraulic conductance measurements, which were made on day 2 of the measurement cycle. Immediately after hydraulic conductance measurements were completed, plant tissue was placed in a chemical fixative and stored until further processing for microscopic analysis. This three-day measurement cycle was continued until all plants had been measured.

Table 1. Leaf characteristics for the five species used in this study. Mean ± SD values for five replicates are shown for grass blade length and the blade width at 50% of the blade length

Species	Blade length (cm)	Blade width (cm)
Ange	30.8 ± 3.4	0.57 ± 0.14
Scsc	27.0 ± 2.9	0.43 ± 0.74
Sonu	38.8 ± 3.1	0.95 ± 0.18
Elca	35.3 ± 5.1	0.87 ± 0.29
Brin	27.2 ± 2.4	0.64 ± 0.14

Gas exchange

The most recently mature leaf blade of each plant was identified and divided into five equal longitudinal sections. The middle of each section was marked (using a black marker) and all subsequent measurements were centred on this mid-point. The distance from the ligule to the centre of each blade section (d_L) was measured for leaf position. *A*, *E*, g_{wv} and leaf temperature (T_{Leaf}) were measured using an Infrared Gas Exchange System (Li-6400, Li-Cor, Inc., Lincoln, NE, USA) with the fluorometer cuvette, which has a smaller chamber size (2 cm^2), to maximize the proportion of the cuvette occupied by the leaf section. Conditions inside the cuvette were maintained to match the condition of the growth chamber [~400 μmol mol^{-1} CO_2, 30 °C, 50 ± 5% relative humidity, 1000 μmol m^{-2} s^{-1} = photosynthetically active radiation (PAR)]. Gas exchange measurements were

first made on the basal section and then sequentially along the length of the blade toward the apex. Data from the Li-6400 was logged every 5 s until both A and g_{wv} were stable for >1 min (typically ~5–10 min of logged data). Data were imported into Matlab (Mathworks, Inc., Natick, MA, USA), visually inspected to ensure stability and then the mean of the last minute of data (12 logged points) was calculated and corrected for the amount of leaf area in the chamber during the measurement.

Hydraulic conductivity

Axial hydraulic conductivity within the xylem (K_X) was determined by measuring the flow rate through a blade segment when exposed to a hydrostatic pressure gradient as described by Sperry, Donnelly & Tyree (1988) for woody stems and modified by Martre, Durand & Cochard (2000) for grass blades. The selected blade from each plant was cut under water and transported to the water reservoir for K_x measurements. An ~40 mm leaf segment was cut under water and wrapped longitudinally around a 1.3 cm silicone rubber rod and each end secured with Teflon tape taking care to leave the cut end of the leaf segment exposed and extending beyond the end of the silicone rod. Each end of the blade section was trimmed with a razor blade immediately prior to placement in a 1.6 cm ID vinyl tube. The basal end of the leaf was connected to a reservoir of degassed de-ionized water filtered (0.2 μm) and pressurized to ~10 kPa. The apical end of the leaf was connected to a reservoir of degassed de-ionized water on a micro-balance (±0.1 mg, Ohaus Pioneer; Ohaus Corporation, Parsippany, NJ, USA) to measure the flow rate of pressurized water through the leaf. Data from the balance were captured via a laptop computer at 1 s intervals and flow rate was calculated as the change in water mass per unit time. Flow was measured on each segment until the rate stabilized (typically ~ 5–10 min), and then 5 min of data were collected to calculate K_x. The temperature of the water bath was also monitored during measurements and K_x of each section was normalized to the viscosity of water at 20 °C.

The background flow rate was also determined before and after measuring the K_x of each blade segment. The pressure on each side of the leaf was equilibrated to eliminate any pressure gradient across the leaf segment and the background flow was measured for 10 min. The average of the two measurements was used in calculations of hydraulic conductivity, and was typically less than 5% of the measured flow rate through the leaf section. Background flow was subtracted from pressurized flow and the result divided by the pressure gradient to yield K_x (mmol mm MPa^{-1} s^{-1}).

Following K_x measurements of all sections of an individual leaf blade, the entire blade (including the sections not used for K_x and gas exchange measurements) was scanned (at 600 dpi, Epson Perfection V500; Epson America Inc., Long Beach, CA, USA) for determination of leaf area (ImageJ; Rasband 1997–2011). K_x was divided by the amount of leaf area distal to each blade section to yield leaf specific hydraulic conductivity K_{x*leaf} (mmol mm^{-1} MPa^{-1} s^{-1}).

Leaf anatomy

Immediately following hydraulic measurements, leaf blade tissue was vacuum infiltrated with a fixative (formalin-acetic acid-alcohol) and placed in 4 °C storage for further processing. Each blade section was divided in half; the basal half was used for determination of stomatal density and the apical half was embedded with paraffin, stained and used for characterization of internal leaf structure. Stomatal density images were taken directly on the leaf blade tissue to avoid errors associated with any stretching that can result during casting. This maximized our potential to identify small differences along individual leaves. Leaf blade tissue was illuminated with 543 nm wavelength (Zeiss lsm5 Pascal confocal microscope; Carl Zeiss MicroImaging, LLC, Peabody, MA, USA) and fluoresced images were taken using a digital camera (Zeiss Axiocam; Carl Zeiss MicroImaging). Each image consisted of eight slices taken at 5 μm increments, which effectively changed the focal length in order to capture all stomata on the undulating surface of the grass blades. Stomatal density was determined on four images per surface (abaxial and adaxial) of each blade section and averaged. The image area was 1.5 mm^2 and stomatal densities are reported in stomata mm^{-2}. Guard cell length was also measured on these same images; the guard cell length of 10 stomata per image was measured (80 guard cells per section) and averaged for each blade section. Stomatal pore index (SPI) was calculated as guard cell length^2 multiplied by stomatal density as a unitless index of maximum stomatal pore area per lamina area (Sack *et al.* 2003).

Blade sections were embedded with paraffin to determine interveinal distance and diffusional path length. Blade segments were embedded with paraffin at the K-State Histology Lab and then double stained with Safranin-O and Fast Green (Ruzin 1999). Images were taken with a digital camera (Leica DFC 290; Leica Microsystems GmbH, Wetzlar, Germany) coupled to a light microscope (Leica DM1000; Leica Microsystems GmbH) and analysed using ImageJ (Rasband 1997–2011). Interveinal distance was determined by measuring the distance between the centroids of two neighbouring vascular bundles, and the mean distance of all measurements per blade segment determined. We calculated an index of the diffusional path length of water movement through the mesophyll (D_m) to estimate the change in extra-xylery resistance along grass blades. As the exact pathway water moves through the mesophyll is still the subject of debate (Westgate & Steudle 1985; Ye, Holbrook & Zwieniecki 2008), we calculated an index of this path length rather than try to estimate the exact distance water must travel from vascular bundle to evaporating site, which we assumed to be near the stomatal pore (Pickard 1981). D_m was determined by measuring the vertical distance (D_v) from each vascular bundle to the

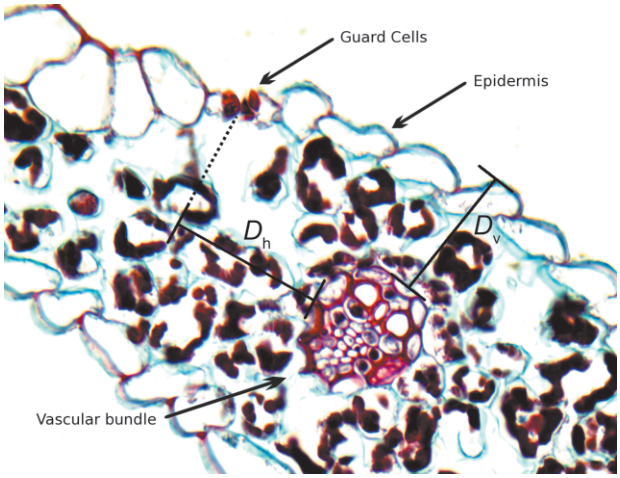

Figure 1. Cross section of an *Elymus canadensis* blade double stained with Safranin-O and Fast Green taken on a light microscope at 40× magnification. Key anatomical characteristics are labelled as well as the measurements used to calculate D_m (Eqn 1). D_v was measured from the top of the vascular bundle to the outer edge of the epidermis, and D_h was measured as the transverse distance from the edge of the vascular bundle to the centre of the stomatal pore.

epidermis, and the horizontal distance (D_h) to the nearest stomatal pore (Fig. 1) then D_m was calculated as:

$$D_m = \sqrt{D_v^2 + D_h^2} \quad (1)$$

For the grass blades measured, stomata were typically arranged in rows associated with each vascular bundle. Because of this structural arrangement, we assumed that the water supplying the cells around the stomatal complex was from the nearest bundle, and so D_h was only measured for the closest stomate.

All statistical analyses were performed using the R open source statistical software package (R Development Core Team 2008). Data were first checked for normality and any outliers removed. Linear regression was used for all analyses of variables with leaf blade position. For comparisons of anatomical features between species, paired *t*-tests were made using the 'Holm' correction for multiple comparisons. To determine the relationship between D_m and g_{wv}, linear mixed-effects model analysis (from the 'nlme' library – Pinheiro *et al.* 2008) was used to minimize variability attributed to individuals (individual was the random variable).

RESULTS

Gas exchange

Stomatal conductance increased acropetally for all species measured. Species within functional groups had similar values and were grouped together for regression analyses (Fig. 2a,b). g_{wv} was generally lower for C_4 species (range: 0.05–0.22 mol $m^{-2} s^{-1}$) compared with C_3 species (0.1–0.45 mol $m^{-2} s^{-1}$), which is expected because of differences in photosynthetic pathways. The acropetal increase in g_{wv} was greater per unit length for the selected C_3 species than for the C_4 species as determined by the slope of the line between d_L and g_{wv} (Fig. 2a,b), but the relative increase was similar between the two functional groups (C_3 – 105%, C_4 – 140%). T_{Leaf} decreased acropetally for C_3 blades as would be expected with increasing g_{wv} (Fig. 2c) but showed no consistent pattern for C_4 blades (Fig. 2d). Smaller increases in g_{wv} for the C_4 species may have been too small to generate temperature differences detectable by the sensor. While g_{wv} always increased acropetally when the angle of the leaf blade was greater than 0° from horizontal, g_{wv} decreased toward the tip when the blade angle was <0° (Fig. 2, red symbols). Data represented by red symbols were not included in the regression analyses. *E* also increased acropetally in all species measured (Fig. 3a,b), but did not increase in direct proportion to g_{wv}. As *E* is a function of g_{wv} and the vapour pressure gradient across the leaf surface, decreases in T_{Leaf} along the blade would reduce the vapour pressure gradient and reduce the acropetal increase in *E*.

Photosynthetic rates (*A*) also increased acropetally; 35 and 100% increases along the leaf blade for C_3 and C_4 grasses, respectively (Fig. 3c,d). C_4 species had greater variability in *A* (1–18 mmol $m^{-2} s^{-1}$) compared with C_3 species (5–15 mmol $m^{-2} s^{-1}$). C_4 species exhibited a greater acropetal increase in *A*, which may have been partly due to the greater variability within the C_4 functional group. As with

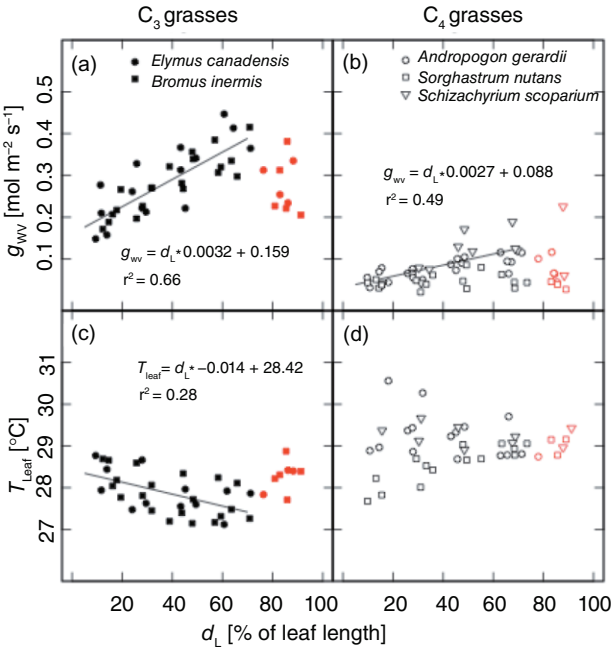

Figure 2. Relationship between stomatal conductance (g_{wv}, panels a and b), leaf temperature (T_{Leaf}, panels c and d) and leaf blade position reported as the percentage of leaf length measured from the ligule. Black symbols are measurements made on leaf sections with an angle >0° from horizontal, red symbols are measurements made where the leaf tip was drooping and leaf angle was <0° from horizontal. g_{wv} increased acropetally for all species when leaf angle was >0°.

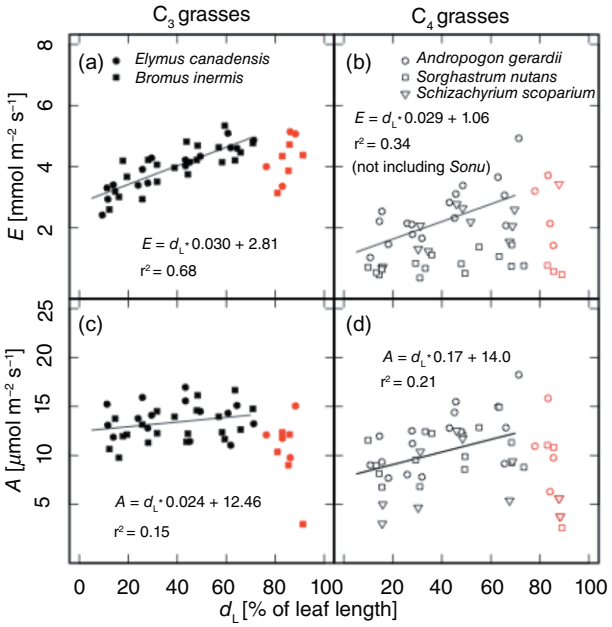

Figure 3. Relationship between transpiration (E, panels a and b), photosynthetic rate (A, panels c and d) and leaf blade position reported as the percentage of leaf length measured from the ligule. Black symbols are measurements made on leaf sections with an angle >0° from horizontal, red symbols are measurements made where the leaf tip was drooping and leaf angle was <0° from horizontal. Data represented by the red symbols were not included in the regression analyses.

g_{wv}, A declined at the tips of the blades when leaf blade angle was <0° from horizontal (Fig. 3c,d, red symbols).

Hydraulic conductivity

The hydraulic efficiency of the leaf xylem remained relatively constant within the blades when normalized for leaf area. Leaf specific hydraulic conductivity in the xylem (K_{x*leaf}, mmol mm^{-1} MPa^{-1} s^{-1}) did not change significantly within blades of any species measured (Fig. 4). So, for a given amount of leaf area, the capacity to move water through the xylem did not change along the blades. The C_4 species selected tended to have higher K_{x*leaf}; *Sonu* had K_{x*leaf} of 1.19, which was significantly greater ($P < 0.01$) than *Ange* (0.90). There was no significant difference in K_{x*leaf} between the other species measured.

Leaf anatomy

Leaf structure varied significantly along the blades of all species measured (Table 2, Fig. 5). Guard cell length increased slightly for *Elca*, but did not change in the other species (Table 2). Both stomatal density and SPI were constant along the blade for all species measured (Table 2). The selected C_3 species had significantly lower stomatal densities than the C_4 species (Table 2); stomatal densities ranged from 30 to 100 mm^{-2} and from 75 to 310 mm^{-2} for C_3 and C_4 species, respectively. The guard cell length, however, was significantly longer for the C_3 species (range 60.36–62.19 μm) than the C_4 species (range 15.62–17.48 μm). SPI varied minimally within each functional group (Table 2), but there were significant differences between C_3 and C_4 species. Significant decreases in interveinal distance (Fig. 5a,b) coupled to constant stomatal density and SPI (Table 2) should lead to shorter distances for water movement from a vascular bundle to stomate. The diffusional distance for water movement, measured as the distance from a vascular bundle to stomatal complex, decreased acropetally in all plants measured in this study (Fig. 5c,d). This decrease in D_m was also related to rates of gas exchange, as there was a significant negative relationship between D_m and g_{wv} (Fig. 6).

DISCUSSION

Functional changes along grass leaves

We have identified a tight correlation between structure and function within individual grass blades across a range of species. A and g_{wv} increased acropetally along the blades of all species measured, which correlated to changes in the hydraulic architecture of blades. Previous studies investigating the heterogeneity of gas exchange in grasses also identified large increases in A and g_{wv} that were correlated with large light gradients from base to tip (Meinzer & Saliendra 1997). In this study, we build on this fundamental work to

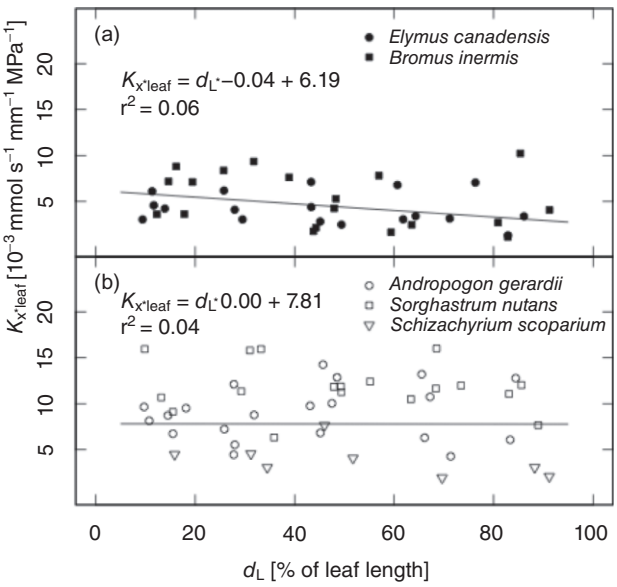

Figure 4. Leaf specific hydraulic conductivity (K_{x*leaf}) as a function of leaf blade position for C_3 (a) and C_4 (b) species. K_{x*leaf} remained relatively constant for all species measured as the linear regression between K_{x*leaf} and leaf position was not significant at the $P < 0.05$ level within a functional group or for any individual species. When K_{x*leaf} of all leaf segments were pooled, *Sonu* had the highest K_{x*leaf} (1.19) followed by *Ange* (0.90) and no significant differences between the other species.

Table 2. Relationship between leaf position and anatomical characteristics within grass blades. Mean ± SD values of all leaf segments for each species are reported. Large interspecies differences were still apparent despite the acropetal variability that was the focus of this study. The slope and *P*-value of the regression between the anatomical variable and leaf position are also shown. The slope of the regression between leaf position and interveinal distance is the most consistently significant relationship

	Stomatal density (mm^{-2})			Guard cell length (μm)			Stomatal pore index			Interveinal distance (mm)		
Species	Mean	Slope	*P*-value	Mean	Slope	*P*-value	Mean	Slope	*P*-value	Mean	Slope	*P*-value
Ange	170.3 ± 52.1[a]	0.06	0.57	16.67 ± 0.87[a]	−10.86	0.19	0.044 ± 0.004[a]	0.0000	0.94	0.11 ± 0.02[a]	−0.0003	<0.001
Scsc	143.8 ± 33.14[a]	0.12	0.59	17.48 ± 1.09[a]	0.46	0.95	0.043 ± 0.009[a]	0.0002	0.44	0.22 ± 0.04[b]	−0.0008	<0.01
Sonu	234.9 ± 49.27[a]	0.00	0.44	15.62 ± 1.36[a]	4.44	0.32	0.056 ± 0.011[a]	0.0000	0.99	0.11 ± 0.01[a]	−0.0003	0.02
Elca	58.6 ± 8.08[b]	0.54	0.49	61.67 ± 5.40[b]	2.31	0.04	0.224 ± 0.048[b]	0.0014	0.19	0.30 ± 0.05[c]	−0.0014	<0.01
Brin	49.8 ± 6.59[b]	0.60	0.48	62.19 ± 3.53[b]	2.34	0.13	0.193 ± 0.032[c]	0.0014	0.12	0.24 ± 0.03[b]	−0.0011	<0.01

a, b and c represent significant differences at the $P < 0.05$ level.

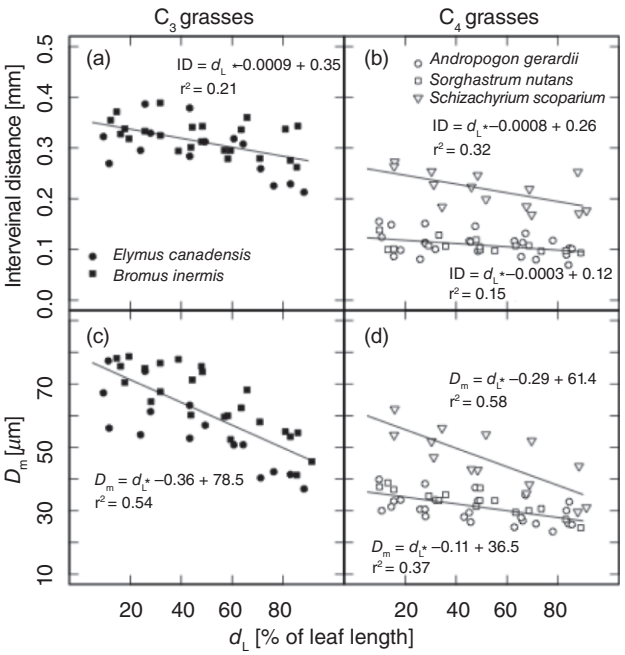

Figure 5. Changes in structural characteristics along grass blades. Interveinal distance (panels a and b) and diffusional path from vascular bundle to stomatal pore (D_m, panels c and d) decreased acropetally for all species in this study. *Ange* and *Sonu* had the smallest change along their blades compared with the other species measured.

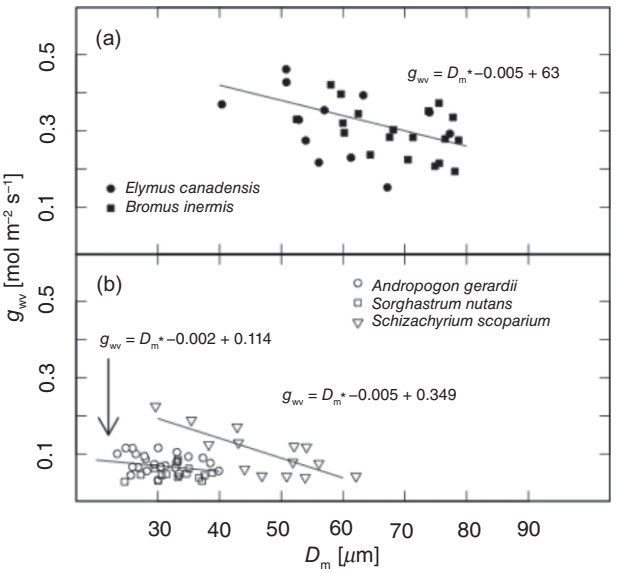

Figure 6. Structure–function relationship within grass leaves of C_3 (a) and C_4 (b) species. D_m is the distance of the diffusional path from vascular bundle to stomatal pore within grass blades. For well-watered plants, g_{wv} is closely related to D_m within individual leaf blades. Analysis was performed using mixed-effects modelling and was significant at the $P < 0.001$ level for pooled C_3 species and *Scsc*, but only significant at the $P < 0.1$ level for *Ange* and *Sonu*.

investigate the relationship between these changing rates of gas exchange in relation to the unique hydraulic architecture of grass leaves.

Our results show stomatal conductance to water vapour (g_{wv}) and carbon assimilation (A) increased acropetally (Figs 2 & 3) for all species measured, which is consistent with previous work (Miranda *et al*. 1981a; Long *et al*. 1989; Meinzer & Saliendra 1997). Despite differences in the absolute values of g_{wv}, the relative increase in g_{wv} was similar between the two functional groups; C_3 species increased by 105% while C_4 species increased by 140%. g_{wv} and A increased acropetally despite no change in light intensity along blades under the growth conditions of this study. The relative increase in A for C_4 plants was greater (100%) than C_3 plants (35%), which is somewhat surprising because C_4 photosynthesis is considered less sensitive to internal CO_2 concentrations due to their ability to concentrate CO_2 at the sites of carboxylation. The steep increase in A for C_4 species is driven, at least in part, by the low photosynthetic rates in the basal sections of the blade for some of the individual C_4 plants (Fig. 3d), which is likely a result of a greater proportion of the leaf consisting of vasculature near the base (Fig. 4). It has been suggested that acropetal increases in A are an adaptation to the growth form of grasses (Long *et al*. 1989) and the measurements of Meinzer & Saliendra (1997) support this idea. If the basal portion of the grass blade is shaded by the tiller and upper leaves, resources will be allocated to the distal regions of leaves to maximize photosynthesis where light availability is typically higher. The native grasses of the tallgrass prairie we selected have relatively narrow leaves and so the effect of shelf-shading may not be as severe as for *Zea mays* and sugarcane (Long *et al*. 1989; Meinzer & Saliendra 1997). Even so, the changes in A and g_{wv} measured here agree with the idea that these grasses have adapted to a growth form where light gradients exist along their blades. It must be noted, however, that acropetal increases in g_{wv} have been found in leaves of tobacco (Nardini *et al*. 2008), which suggests that the systematic changes in gas exchange along leaves are not exclusive to monocots. This pattern of increasing rates of gas exchange may be a fundamental consequence of moving water through a series of channels that exists in all growth forms. Measurements on a wider set of species with a range of growth characteristics would be valuable in further understanding the patterns of gas exchange in leaves.

What then is the underlying mechanism(s) driving increased in g_{wv} along grass leaves? Plants tend to adjust stomatal conductance to maintain the CO_2 concentration inside the leaf (c_i) at an optimal level across a range of conditions (Cernusak & Marshall 2001). Mott and Buckley (1998) suggested that the maintenance of c_i is a likely signal for the control of 'patchy' stomatal conductance within the individual. The increase in g_{wv} along grass blades could exist to maintain c_i at an optimum level for the increasing rates of photosynthesis. We can evaluate this mechanism as the driver of acropetal increases in g_{wv} for this study with a simple modelling exercise based on established equations. Using A and g_{wv} calculated from the linear regressions for C_3 leaves (Figs 2 & 3) and converting g_{wv} to stomatal conductance for CO_2 ($g_c = g_{wv}/1.6$), we can calculate c_i by rearranging the linear equation for photosynthesis:

$$A = g_c (c_a - c_i) \tag{2}$$

where c_a was set to 400 μmol mol^{-1} (conditions inside the chamber during gas exchange measurements). This simple modelling approach assumes that boundary layer conductance is large compared with g_{wv} and that changes in conductance along the leaf are driven by changes in g_{wv}. This assumption is valid for the conditions of this study, as boundary layer conductance was ~2 orders of magnitude greater than g_{wv} during gas exchange measurements (data not shown). In order to maintain a constant c_i, the modelled increase in g_{wv} was 35% acropetally along the blade, which is a smaller increase than we measured for C_3 leaves. This suggests that the changes in A and g_{wv} observed in this study would lead to increases in c_i along the leaves in the species measured. This is the opposite trend compared with field-grown sugarcane (Meinzer & Saliendra 1997), where c_i values decreased acropetally. The difference in c_i patterns may be due, in part, to the different photosynthetic pathways utilized by the plants of interest. Our modelling exercise was carried out for C_3 grasses, which have photosynthetic rates that saturate at higher c_i values than C_4 plants (like sugarcane) and may have a relatively larger change in g_{wv} to maintain higher levels of c_i. Measurement conditions may also contribute to the different patterns of c_i in our model compared with the results from sugarcane. Changes in the rates of gas exchange for sugarcane were measured in the presence of large light gradients along the blades, our measurements were made on leaves growing with a uniform light environment along the blades. The increased light availability along sugarcane blades may change the pattern of g_{wv} compared with our results. The range of A values measured along grass blades, however, was quite similar between the two studies, and so it is unclear how leaf-level light gradients would have affected our results. Finally, it is also possible that some unknown 'signal' besides c_i results in g_{wv} adjustments and may have driven the increase in stomatal conductance we observed. Further work needs to be done comparing C_3 and C_4 patterns of g_{wv} and A along leaves under a range of conditions (e.g. light gradients, boundary layer gradients, etc.).

Structural changes along grass leaves

Water flow within leaves can be divided into two broad structural categories: flow within the xylem, and flow outside the xylem as water moves out of the vascular bundle to sites of evaporation. The capacity for water movement within the xylem, calculated as leaf specific hydraulic conductivity (K_{x*leaf}, mmol mm^{-1} s^{-1} MPa^{-1}), remained relatively constant (Fig. 4) along the grass blades, which is consistent with other studies of grass hydraulic architecture (Martre &

Durand 2001). Martre & Durand (2001) showed K_{x*leaf} increased along the sheath, but then remained constant along the blade with a slight increase in the tips using leaves of *Festuca arundinacea* Schreb cv. Clarine. Similarly, others have identified reductions in hydraulic conductivity and total vessel area along grass blades as leaf area declines (Colbert & Evert 1982; Russell & Evert 1985; Dannenhoffer *et al*. 1990), but in these studies leaf specific hydraulic conductance was not reported.

The conductance of water outside the xylem (K_{ox}, mmol mm s^{-1} MPa^{-1}) can be a significant source of resistance within leaves (Martre, Cochard & Durand 2001; Cochard *et al*. 2004; Mott 2007) and has been related to the internal structure of the leaves (Sack & Frole 2006; Brodribb *et al*. 2007). Increases in vascular density coupled to constant or increasing stomatal density resulted in shorter path lengths (D_m) for the movement of water from vascular bundles to the site of evaporation (Fig. 5). Vascular density also increased in *F. arundinacea* (Martre & Durand 2001) but was less variable in 7-day-old *Zea mays L.* (Miranda, Baker & Long 1981b), where interveinal distances remained constant over most of the leaf. Based on previous findings (Sack & Frole 2006; Brodribb *et al*. 2007), the decrease in D_m acropetally found here would reduce the resistance to water movement outside the xylem facilitating greater g_{wv} in distal portions of grass leaves without drastic increases in the $\Delta\Psi$ from vascular bundle to site of evaporation. Increases in the K_{ox} along grass blades while K_{x*leaf} remains constant changes the relative proportions of these conductances within individual leaves and may facilitate the increase in g_{wv} along grass blades, but much work remains on the complex relationship of liquid and vapour phase resistances within leaves (Meinzer 2002) to fully understand these increases in g_{wv} along grass blades.

Implications

Despite the uncertainty of the mechanism controlling g_{wv}, it is apparent that there is a tight correlation between hydraulic architecture and rates of gas exchange within leaves of grasses. The changes in architecture likely minimize the water potential gradients within the leaf as the rate of water loss increases acropetally. Assuming D_m to be directly proportional to leaf conductance outside the xylem (Sack & Frole 2006; Brodribb *et al*. 2007), we used an electrical analogue approach to model the effect of changes in extra-xylery conductance on the water potential gradient from vascular bundle to the epidermis ($\Delta\Psi_{vb\text{-}e}$). $\Delta\Psi_{vb\text{-}e}$ was calculated along the blade as:

$$\Delta\Psi_{vb-e} = \frac{E}{K_{ox}} * l \quad (3)$$

where K_{ox} (mmol mm s^{-1} MPa^{-1}) is the hydraulic conductance outside the xylem from vascular bundle to epidermis and l is equal to D_m for this exercise. We set K_{ox} to an arbitrary value of 0.7 mmol mm s^{-1} MPa^{-1} (which is one-tenth the value of measured axial hydraulic conductance) and was assumed to be constant along the leaf so that only E and l changed according to our measurements on C_3 leaves. The absolute value of K_{ox}, however, is not important for this simulation because we are interested in the effect of changing D_m on $\Delta\Psi_{vb\text{-}e}$ from vascular bundle to epidermis as g_{wv} increases. Using this approach, the advantage of decreasing D_m as g_{wv} increases is apparent (Fig. 7), as the relative change in $\Delta\Psi_{vb\text{-}e}$ was 63% less at the leaf tip than if there was no acropetal change in D_m. This suggests that the structural change in grass leaves minimizes the water potential gradients across the leaf mesophyll as g_{wv} increases. The hydraulic conductance through both xylem and mesophyll (K_{leaf}) has been shown to decrease acropetally in tobacco leaves (Nardini *et al*. 2008) and was inversely related to g_{wv}. Nardini *et al*. (2008) suggest that g_{wv} would increase as K_{leaf} decreased to maintain a constant Ψ_{leaf}, as no significant difference in Ψ_{leaf} was identified between basal and apical leaf sections in their study. While it is unlikely that Ψ_{leaf} remained constant along grass blades in this study due to the need for a water potential gradient to exist to move water from the base to tip (Zwieniecki *et al*. 2002), g_{wv} may still be increasing to minimize changes in leaf water status as K_{leaf} decreases along grass blades.

Our results highlight the tight correlation between the structure and function within individual grass blades. The increasing rates of photosynthesis along grass blades demand greater g_{wv} in order to maintain c_i values at an optimum level. Decreases in the extra-xylery resistance to water movement should allow faster transport of water without increasing water potential gradients from vascular

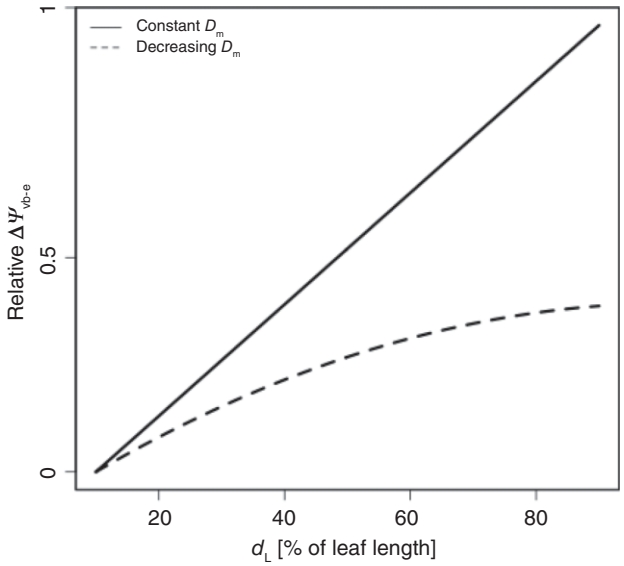

Figure 7. The modelled change in water potential gradient between the vascular bundle to epidermis ($\Delta\Psi_{vb\text{-}e}$) for a C_3 grass blade. The solid line represents the increase in $\Delta\Psi_{vb\text{-}e}$ assuming no acropetal change in D_m. When D_m decreased, as observed for C_3 grass blades in this study, the increase in $\Delta\Psi_{vb\text{-}e}$ was 63% less than when D_m remained constant along the blade.

bundles to the site of evaporation. This coupling of structure and function allow the often long, narrow leaves of monocots to maximize resources while minimizing pressure gradients along the blades.

ACKNOWLEDGMENTS

We greatly appreciate the technical assistance of Whitley Jackson and Johanna Burniston; the expertise of Dr. Dan Boyle in helping in florescence microscope imaging; and Dr. Kendra McLauchlan for the use of laboratory facilities. We would also like to thank the two anonymous reviewers for their thoughtful comments, which improved an earlier version of this manuscript. The Kansas Technology Enterprise Corporation and the Konza Prairie LTER (DEB-0823341) provided financial support.

REFERENCES

Affek H., Krisch M. & Yakir D. (2006) Effects of intraleaf variations in carbonic anhydrase activity and gas exchange on leaf $C^{18}OO$ isoflux in *Zea mays*. *The New Phytologist* **169,** 321–329.

Brodribb T.J., Holbrook N.M., Zwieniecki M.A. & Palma B. (2005) Leaf hydraulic capacity in ferns, conifers and angiosperms: impacts on photosynthetic maxima. *The New Phytologist* **165,** 839–846.

Brodribb T.J., Feild T.S. & Jordan G.J. (2007) Leaf maximum photosynthetic rate and venation are linked by hydraulics. *Plant Physiology* **144,** 1890–1898.

Buckley T., Farquhar G. & Mott K. (1999) Carbon-water balance and patchy stomatal conductance. *Oecologia* **118,** 132–143.

Buckley T.N. & Mott K.A. (2000) Stomatal responses to non-local changes in PFD: evidence for long-distance hydraulic interactions. *Plant, Cell & Environment* **23,** 301–309.

Cernusak L.A. & Marshall J.D. (2001) Responses of foliar $\delta^{13}C$, gas exchange and leaf morphology to reduced hydraulic conductivity in *Pinus monticola* branches. *Tree Physiology* **21,** 1215–1222.

Cochard H., Nardini A. & Coll L. (2004) Hydraulic architecture of leaf blades: where is the main resistance? *Plant, Cell & Environment* **27,** 1257–1267.

Colbert J. & Evert R. (1982) Leaf vasculature in sugarcane (*Saccharum-officinarum L*). *Planta* **156,** 136–151.

Dannenhoffer J., Ebert W. & Evert R. (1990) Leaf vasculature in barley, *Hordeum vulgare* (*Poaceae*). *American Journal of Botany* **77,** 636–652.

Helliker B.R. & Ehleringer J.R. (2000) Establishing a grassland signature in veins: O-18 in the leaf water of C-3 and C-4 grasses. *Proceedings of the National Academy of Sciences of the United States of America* **97,** 7894–7898.

Long S., Bolharnordenkampf H., Croft S., Farage P., Lechner E. & Nugawela A. (1989) Analysis of spatial variation in CO_2 uptake within the intact leaf and its significance in interpreting the effects of environmental-stress on photosynthesis. *Philosophical Transactions of the Royal Society of London. Series B, Biological Sciences* **323,** 385–395.

Marenco R.A., Siebke K., Farquhar G.D. & Ball M.C. (2006) Hydraulically based stomatal oscillations and stomatal patchiness in *Gossypium hirsutum*. *Functional Plant Biology* **33,** 1103–1113.

Martre P. & Durand J.L. (2001) Quantitative analysis of vasculature in the leaves of *Festuca arundinacea* (Poaceae): implications for axial water transport. *International Journal of Plant Sciences* **162,** 755–766.

Martre P., Durand J.L. & Cochard H. (2000) Changes in axial hydraulic conductivity along elongating leaf blades in relation to xylem maturation in tall fescue. *The New Phytologist* **146,** 235–247.

Martre P., Cochard H. & Durand J.L. (2001) Hydraulic architecture and water flow in growing grass tillers (*Festuca arundinacea* Schreb.). *Plant, Cell & Environment* **24,** 65–76.

Meinzer F.C. (2002) Co-ordination of vapour and liquid phase water transport properties in plants. *Plant, Cell & Environment* **25,** 265–274.

Meinzer F.C. & Saliendra N.Z. (1997) Spatial patterns of carbon isotope discrimination and allocation of photosynthetic activity in sugarcane leaves. *Australian Journal of Plant Physiology* **24,** 769–775.

Miranda V., Baker N. & Long S. (1981a) Limitations of photosynthesis in different regions of the *Zea-mays* leaf. *The New Phytologist* **89,** 179–190.

Miranda V., Baker N. & Long S. (1981b) Anatomical variation along the length of the Zea-mays leaf in relation to photosynthesis. *The New Phytologist* **88,** 595–605.

Mott K.A. (2007) Leaf hydraulic conductivity and stomatal responses to humidity in amphistomatous leaves. *Plant, Cell & Environment* **30,** 1444–1449.

Mott K.A. & Buckley T.N. (1998) Stomatal heterogeneity. *Journal of Experimental Botany* **49,** 407–417.

Nardini A., Gortan E., Ramani M. & Salleo S. (2008) Heterogeneity of gas exchange rates over the leaf surface in tobacco: an effect of hydraulic architecture? *Plant, Cell & Environment* **31,** 804–812.

Ogee J., Cuntz M., Peylin P. & Bariac T. (2007) Non-steady-state, non-uniform transpiration rate and leaf anatomy effects on the progressive stable isotope enrichment of leaf water along monocot leaves. *Plant, Cell & Environment* **30,** 367–387.

Pickard W.F. (1981) How does the shape of the substomatal chamber affect transpirational water loss? *Mathematical Biosciences* **56,** 111–127.

Pinheiro J., Bates D., DebRoy S., Sarkar D. & the R Core team (2008) nlme: linear and nonlinear mixed effects models. R package version 3.1-90.

R Development Core Team (2008) *R: A Language and Environment for Statistical Computing*. R Foundation for Statistical Computing, Vienna, Austria. ISBN 3-900051-07-0, URL http://www.R-project.org.

Rasband W.S. (1997–2011) *ImageJ*. U. S. National Institutes of Health, Bethesda, Maryland, USA. URL http://imagej.nih.gov/ij/.

Russell S. & Evert R. (1985) Leaf vasculature in *Zea-mays*-L. *Planta* **164,** 448–458.

Ruzin S.E. (1999) *Plant Microtechnique and Microscopy*. Oxford University Press, New York, USA.

Sack L. & Frole K. (2006) Leaf structural diversity is related to hydraulic capacity in tropical rain forest trees. *Ecology* **87,** 483–491.

Sack L., Cowan P.D., Jaikumar N. & Holbrook N.M. (2003) The 'hydrology' of leaves: co-ordination of structure and function in temperate woody species. *Plant, Cell & Environment* **26,** 1343–1356.

Sperry J., Donnelly J. & Tyree M. (1988) A method for measuring hydraulic conductivity and embolism in xylem. *Plant, Cell & Environment* **11,** 35–40.

West G.B., Brown J.H. & Enquist B.J. (1999) A general model for the structure and allometry of plant vascular systems. *Nature* **400,** 664–667.

Westgate M.E. & Steudle E. (1985) Water transport in the midrib tissue of maize leaves: direct measurement of the propagation of changes in cell turgor across a plant tissue. *Plant Physiology* **78,** 183–191.

Ye Q., Holbrook N.M. & Zwieniecki M.A. (2008) Cell-to-cell pathway dominates xylem-epidermis hydraulic connection in *Tradescantia fluminensis* (Vell. Conc.) leaves. *Planta* **227,** 1311–1319.

Zwieniecki M.A., Melcher P.J., Boyce C.K., Sack L. & Holbrook N.M. (2002) Hydraulic architecture of leaf venation in *Laurus nobilis* L. *Plant, Cell & Environment* **25,** 1445–1450.

Received 15 September 2011; received in revised form 15 November 2011; accepted for publication 20 November 2011